cause of the trigonal distortion in the aluminum alums. However, one would not expect the Cr^{3+} to bond to its surroundings in the same manner as Al^{3+} or Ga^{3+} since the latter two ions have closed electron shells. The best one can say at this stage is that many of the atoms in the unit cell can contribute to the trigonal distortion of the chromium complexes, and it is not certain which of Van Vleck's first two postulates is operative. Additional data on the physical behavior of the chromium magnetic complexes are obtained from ENDOR studies, which is the subject of Paper II.[4]

[1]D. M. S. Bagguley and J. H. E. Griffiths, Proc. Roy. Soc. (London) A204, 188 (1950).
[2]B. Bleaney, Proc. Roy. Soc. (London) A204, 203 (1950).
[3]J. M. Baker, Proc. Phys. Soc. (London) B69, 633 (1956).
[4]A. Danilov and A. Manoogian, following paper, Phys. Rev. B 6, 4103 (1972).
[5]G. S. Bogle, J. R. Gabriel, and G. A. Bottomly, Trans. Faraday Soc. 53, 1058 (1957).
[6]J. M. Daniels and H. Wesemeyer, Can. J. Phys. 36, 144 (1958).
[7]G. Burns, Phys. Rev. 123, 1634 (1961).
[8]R. W. Schwartz and R. L. Carlin, J. Am. Chem. Soc. 92, 6763 (1970).
[9]H. Lipson and C. A. Beevers, Proc. Roy. Soc. (London) A148, 664 (1935).
[10]H. Lipson, Proc. Roy. Soc. (London) A151, 347 (1935).
[11]D. T. Kromer, M. I. Kay, and A. C. Larson, Acta Cryst. 22, 182 (1967).
[12]A. H. C. Ledsham and H. Steeple, Acta Cryst. B24, 1287 (1968).
[13]A. H. C. Ledsham and H. Steeple, Acta Cryst. B24, 320 (1968).
[14]H. P. Klug and G. L. Kieffer, J. Am. Chem. Soc. 62, 2071 (1940).
[15]P. M. Llewellyn, P. E. Whittlestone, and J. M. Williams, J. Sci. Instr. 39, 586 (1962).
[16]C. P. Slichter, Phys. Rev. 99, 479 (1955).
[17]B. Bleaney and K. D. Bowers, Proc. Phys. Soc. (London) A65, 1135 (1951)
[18]A. Manoogian and A. G. Danilov, Can. J. Phys. 48, 1448 (1970).
[19]B. R. McGarvey, J. Chem. Phys. 40, 809 (1964).
[20]J. H. Van Vleck, J. Chem. Phys. 7, 61 (1939).

PHYSICAL REVIEW B VOLUME 6, NUMBER 11 1 DECEMBER 1972

Electron-Nuclear Double Resonance of $^{53}Cr^{3+}$ in Gallium Alums. II

A. G. Danilov and A. Manoogian
Department of Physics, University of Ottawa, Ottawa KIN 6N5, Canada
(Received 22 May 1972)

Electron-nuclear-double-resonance (ENDOR) studies are reported for the isotope $^{53}Cr^{3+}$ enriched to 96% in the gallium alums $RbGa(SO_4)_2 \cdot 12H_2O$ and $CsGa(SO_4)_2 \cdot 12H_2O$, including their deuterated forms. All measurements were made at 4.2 °K and at *X*-band microwave frequencies (~ 9.4 GHz). The study allowed accurate values of the various hyperfine parameters to be determined and ENDOR patterns to be classified. The hyperfine parameters *A* and *B* had the relationships $A > B$ in RbGa alum and $A < B$ in CsGa alum. A model for the behavior of the alums as a function of temperature is postulated, with the result that the quadrupole moment of ^{53}Cr is determined to be $eQ = -0.035 \pm 0.005$ b. The magnetic moment of $^{53}Cr^{3+}$ was found to be approximately $-0.464\mu_N$ which is slightly lower than the accepted value. The effect of deuteration did not show significant differences from the hydrated alums. ENDOR transitions are observed relating three adjacent hyperfine levels of ^{53}Cr instead of the usual two. Possible mechanisms for this effect are qualitatively discussed.

I. INTRODUCTION

Electron-nuclear-double-resonance (ENDOR) experiments were carried out on chromium-doped alums in order to obtain more information about their physical behavior. The study was done on the gallium alums $RbGa(SO_4)_2 \cdot 12H_2O$ and $CsGa(SO_4)_2 \cdot 12H_2O$, including their deuterated forms. The chromium dopant was 96%-enriched $^{53}Cr^{3+}$ and its concentration in the samples was estimated to be less than 0.01 wt %. The crystals were grown from saturated solutions of the constituent sulfates by slow evaporation at room temperature. They were colorless and had dimensions of about $4 \times 3 \times 2$ mm. All measurements were done at a temperature of 4.2 °K and at *X*-band microwave frequencies (9.4 GHz).

No ENDOR work on the alums has been previously reported, but the rather varied paramagnetic behavior of alums provides motivation for further study by this technique. This is especially true at low temperatures where many of the alums

appear to behave anomalously. The study allows a more complete description of the chromium magnetic complexes than is possible by ordinary ESR. The anisotropy of the hyperfine interaction, which is an important quantity, can be readily determined. The chromium nuclear g value can also be determined, but with less accuracy. Calculations can be made regarding the nuclear quadrupole moment of ^{53}Cr, but the calculation is not straightforward in that it depends on postulating a model for the behavior of the alums.

The ENDOR of $^{53}Cr^{3+}$ was studied[1,2] extensively some ten years ago in ruby crystals. In the study the hyperfine interaction was assumed to be isotropic and no attempt was made to measure the probable anisotropy. The nuclear quadrupole moment of ^{53}Cr was calculated to be -0.03 b on the basis of several assumptions. The principal assumption was that the electric field gradient at a chromium site in ruby is the same as that at an aluminum site. In a theoretical treatment of the properties of ruby Artman and Murphy[3] have used the method of lattice sums to evaluate the ruby spectral parameters. In regard to the chromium magnetic complexes they assumed that the size difference of 0.1 Å between Cr^{3+} and Al^{3+} creates a local axial distortion, and they postulate a detailed model for the distortion which involves a number of atoms about the chromium site. On this basis they calculated the nuclear quadrupole moment of ^{53}Cr to be $+0.024$ b. In a later paper Artman[4] calculated the electric field gradients of transition-metal sesquioxides which are isomorphous with corundum and concluded that only the absolute value of the ^{53}Cr nuclear quadrupole moment could be calculated. He calculated a value of 0.026 b and stated further that the expected value should fall within the range 0.02–0.05 b.

II. EQUIPMENT AND EXPERIMENTAL PROCEDURE

The spectrometer used in the ENDOR work was the same as shown in Fig. 1 of Paper I.[5] The ENDOR power for inducing nuclear transitions was produced by a Radiometer-Copenhagen No. 127 oscillator followed by two wideband amplifiers producing a total of 3 W of power. However, only a fraction of this power was delivered to the ENDOR coil because of mismatch between the coil and amplifiers. Nevertheless, sufficient power was available to perform ENDOR. The ENDOR coil consisted of three turns of copper wire inside a rectangular TE_{014} sample cavity. The cavity system is shown in Fig. 1. The sample holder was made of Delrin, which is a mixture of Teflon and nylon. This material has both strength and low dielectric loss. The ENDOR coil is wrapped around the center portion of the holder in a groove cut by a fine saw blade. The sample holder is positioned in the cavity at room temperature by observing the center-line position of the coil groove through three small holes drilled in one side of the cavity wall at a distance of $\frac{1}{2}\lambda_g$ from the cavity bottom, and it is then locked into position by a nylon screw threaded into one end. The cavity was cut at the $\frac{3}{4}\lambda_g$ position from the cavity bottom to give easy access for placing of crystals in the

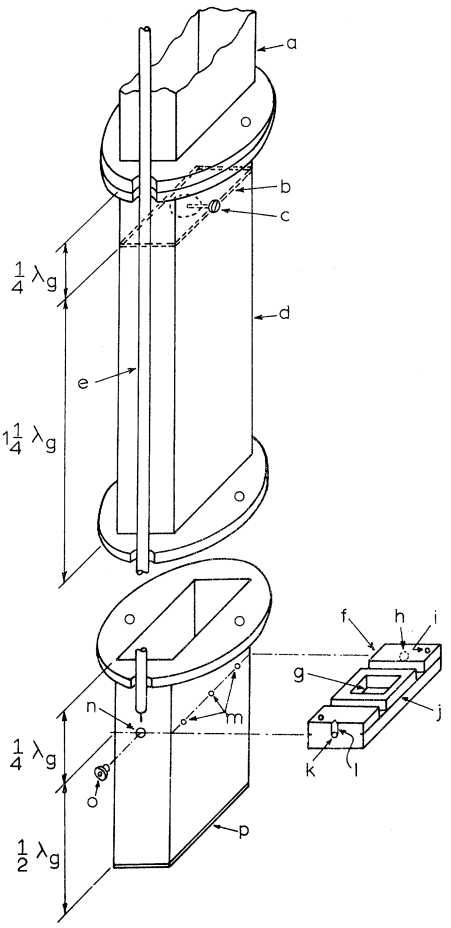

FIG. 1. ENDOR cavity system. (a) Stainless-steel waveguide, (b) iris with $\frac{1}{4}$-in. hole in the center, (c) impedance-matching screw, (d) copper-coated-brass waveguide cavity, (e) coax consisting of a stainless-steel outer tube and an inner copper wire separated by dielectric material, (f) sample holder, (g) sample position in holder, (h) tapped hole in one end of sample holder to take nylon screw for locking holder to cavity wall, (i) two small tapped holes near opposite ends of holder to take temporary screws for lowering and manipulating holder in cavity, (j) saw cut with fine blade on each side of holder, (k) hole in end of holder to pass leads of ENDOR coil, (l) groove to allow coil lead wires to be folded up when placing holder in cavity, (m) three holes in side of cavity to observe center of holder for alignment, (n) hole for coil lead wires to pass through, (o) Perspex plug with hole in center to keep coil lead wires from touching cavity, and (p) cavity bottom plate.

holder. The cavity bottom plate and iris are soldered into place. A matching screw is placed just above the iris hole and its length is such that its end extended to the center of the iris hole when it was screwed tight against the cavity wall. This arrangement ensures that the cavity is always matched, even at 4.2 °K. The loaded Q of the cavity was greater than 4000.

The procedure used to obtain ENDOR was as follows: The ESR spectrum was first obtained with a power level of about 0.02 mW in the cavity and the magnetic field was set on the center of a particular hyperfine line as well as could be estimated. The microwave power was then turned up to about 2 mW, thereby partially saturating the ESR transition. The 200-Hz magnetic field modulation was switched off and power was applied to the ENDOR coil. The power was slowly swept in frequency by a motor drive on the oscillator and it was frequency modulated at 200-Hz by a signal from the phase-sensitive detector (p. s. d.). The frequency sweep rate was about 1 MHz/min and the FM deviation was 75 kHz. The p. s. d. time constant was 1 or 3 sec. After the ENDOR lines were obtained for a given ESR line the magnetic field was adjusted slightly so as to maximize the signals, thereby ensuring that the field value was at the center of the ESR line. The microwave power was then adjusted to maximize the ENDOR signal intensity by obtaining the correct saturation level. Frequency measurements were made by setting the ENDOR signal generator manually to the centers of the transitions, and then switching off the FM modulation. The frequency was then read off a digital counter to the nearest 100 Hz.

III. SPIN HAMILTONIAN

The ground state of $^{53}Cr^{3+}$ is described by the quantum numbers $S=\frac{3}{2}$ and $I=\frac{3}{2}$. The spectrum of each chromium complex consists of three groups of four hyperfine lines. The degree of resolution of the hyperfine lines depends on the particular crystal under study, the dilution of the chromium impurity, and on the perfection of the crystals grown. The spin Hamiltonian used to describe the ENDOR results is of the form

$$\begin{aligned}\mathcal{H}_s = {} & g_{\parallel}\mu_B S_z H_z + g_{\perp}\mu_B (S_x H_x + S_y H_y) + D[S_z^2 - \tfrac{1}{3}S(S+1)] \\ & + AS_z I_z + B(S_x I_x + S_y I_y) + Q'[I_z^2 - \tfrac{1}{3}I(I+1)] \\ & - g'_{n\parallel}\mu_N I_z H_z - g'_{n\perp}\mu_N (I_x H_x + I_y H_y) . \end{aligned} \quad (1)$$

The Hamiltonian for ^{53}Cr is represented by a 16×16 matrix. The first three terms of Eq. (1) are the usual fine-structure terms used in ESR. The forth and fifth terms describe the hyperfine interaction, the sixth term the quadrupole interaction, and the seventh and eighth terms the nuclear Zeeman effect. The last five terms are important in ENDOR since they describe the hyperfine structure. The angular variation of all the terms in Eq. (1) is described in a set of Varian notes.[6]

A. Hyperfine Interaction

The hyperfine terms $AS_z I_z + B(S_x I_x + S_y I_y)$ in the spin Hamiltonian arise from the following terms in the original Hamiltonian:

$$-2g_n\mu_N\mu_B\sum_i\left(\frac{\vec{I}\cdot\vec{s}_i}{r_i^3} - \frac{3(\vec{I}\cdot\vec{r}_i)(\vec{s}_i\cdot\vec{r}_i)}{r_i^5} - \frac{8\pi}{3}\delta(r_i)(\vec{s}_i\cdot\vec{I})\right) . \quad (2)$$

As shown by McGarvey,[7] first-order perturbation theory gives the following expressions for A and B:

$$A = P[\tfrac{4}{21}(1 - 2a^2 + b^2) - K] , \quad (3)$$

$$B = P[-\tfrac{2}{21}(1 - 2a^2 + b^2) - K] , \quad (4)$$

where $P = 2g_n\mu_N\mu_B(1/r^3)$ and K is a parameter resulting from the last term in Eq. (2). For octahedral symmetry of the coordinated ligands we have $a^2=\frac{2}{3}$, $b^2=\frac{1}{3}$, and $1-2a^2+b^2=0$, giving $A=B$ from Eqs. (3) and (4). If $a^2<\frac{2}{3}$ and $b^2>\frac{1}{3}$ then $1-2a^2+b^2$ takes on positive values, giving $A<B$. McGarvey[7] points out that this situation indicates a polarization of electronic charge on the chromium ion due to the six oxygen atoms surrounding the chromium ion being distorted from an octahedral configuration by compression along the trigonal axis. McGarvey[8] shows further in the theory of the spin Hamiltonian describing a trigonal distortion that the D parameter is negative for $a^2<\frac{2}{3}$. For $a^2>\frac{2}{3}$ and $b^2<\frac{1}{3}$ then $1-2a^2+b^2$ takes on negative values, giving $A>B$. McGarvey[8] shows that $a^2>\frac{2}{3}$ corresponds to a positive D value. If the previous case represents a trigonal compression of the coordinated octahedron then the latter case presumably represents a trigonal extension.

B. Quadrupole Interaction

The nuclear-quadrupole-interaction constant Q' in the spin Hamiltonian can be written

$$Q' = \frac{3V_{zz}eQ}{4I(2I-1)}(1-\gamma_\infty) , \quad (5)$$

where V_{zz} is the electric field gradiant external to the chromium ion, eQ is the quadrupole moment of ^{53}Cr, and $1-\gamma_\infty$ is the Sternheimer antishielding factor for Cr^{3+}. Sternheimer[9] has recently estimated $1-\gamma_\infty$ for Cr^{3+} to be 12.0 ± 1.0, and he has also shown[10] that $1-\gamma_\infty=3.36$ for Al^{3+}.

C. Nuclear Zeeman Interaction

The magnetic field as seen by the nucleus is in general not simply the applied external field H. When the field is applied the electronic wave func-

tion is changed by an amount proportional to H, the effect of which modifies the electronic field at the nucleus and results in a paramagnetic shielding. This interaction is called the pseudonuclear Zeeman effect. The magnetic shielding of the nucleus can be treated phenomenologically as done by Geschwind[11] by writing $H(1+\sigma)$ in place of H, where σ is the shielding parameter. Experimentally, $H(1+\sigma)$ is manifested as an effective nuclear g value written g_n'. The effect of shielding modifies the true nuclear g factor g_n by the relation $g_n = g_n'/(1+\sigma)$. One can calculate σ according to Geschwind's formula

$$\sigma = -5.84\langle 1/r^3\rangle_{\text{a.u.}}(\Delta g/\lambda) , \tag{6}$$

where Δg is the electronic g-value shift from 2.0023, λ is the spin-orbit coupling parameter for Cr^{3+} in units of cm^{-1}, and $\langle 1/r^3\rangle$ is the average value of $1/r^3$ for the Cr^{3+}-$3d$ wave function.

D. Relationship between D and V_{zz}

By considering the crystal field at the Cr^{3+} site to consist of a sum of a cubic and an axial part one can obtain the following linear relationship[12-14] between the spin-Hamiltonian parameter D and the electric field gradient V_{zz} due to charges and dipoles external to the chromium ion:

$$D = \tfrac{3}{7}(\lambda/\Delta E)^2\langle r^2\rangle V_{zz} . \tag{7}$$

The quantity $\langle r^2\rangle$ is the average value of r^2 for the Cr^{3+}-$3d$ wave function, λ is the spin-orbit coupling constant, and ΔE is the energy separation between the ground state $^4A_2$ and the excited state $^4T_2$. Equation (7) is approximate in that the smaller effects due to fourth-order terms in the crystal field potential and the contribution of $^2T_2$ excited states are neglected. The effects due to covalent bonding are also neglected.

IV. RESULTS

The alums are referred to below in shortened notation as $Rb(H_2O)$, $Rb(D_2O)$, etc. The $^{53}Cr^{3+}$ hyperfine lines in $Rb(H_2O)$ alum were unresolved at 300 °K but were fairly well resolved at 4.2 °K. This effect is shown in Fig. 2 for the $\Delta M_s = -\frac{3}{2} \rightarrow -\frac{1}{2}$ group of hyperfine lines. The lines in $Rb(D_2O)$ alum were unresolved at both temperatures, while those of $Cs(H_2O)$ and $Cs(D_2O)$ alums were always resolved. In none of the cases did the effect of deuteration reduce the linewidths. However, it is not necessary to have resolution to perform ENDOR. But if the lines are resolved one is able to quickly set the magnetic field at the center of a hyperfine line in order to obtain the desired ENDOR frequencies. The analysis of $Rb(D_2O)$ alum is done by observing the intensities of the ENDOR lines when the magnetic field position is moved in steps across an unresolved group of hyperfine lines. The patterns obtained are then compared with those from $Rb(H_2O)$ alum. It is possible to do this because the intensity patterns are found to be the same in both cases. The ENDOR intensity patterns are the same in $Cs(H_2O)$ and $Cs(D_2O)$ alums, but they differ from those of the Rb alums.

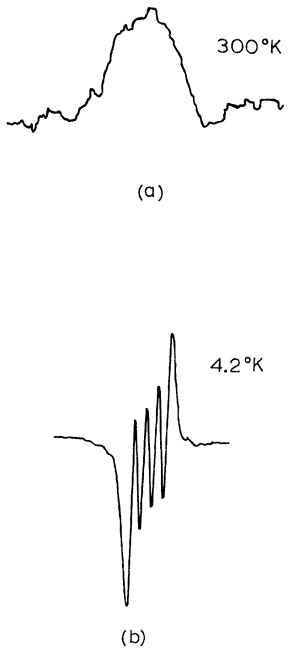

FIG. 2. $\Delta M_s = -\frac{3}{2} \rightarrow -\frac{1}{2}$ group of hyperfine lines of $^{53}Cr^{3+}$ in $RbGa(SO_4)_2 \cdot 12H_2O$ at (a) 300 °K and (b) 4.2 °K.

The mean positions of the groups of hyperfine lines, when the magnetic field is directed along the z and perpendicular directions of a magnetic complex, are the same as those obtained for the even chromium isotope in Paper I.[5] Hence the values of $g_\parallel$, $g_\perp$, and D obtained for the even isotope apply to the case of the odd isotope. The sign of D was also verified to be the same.

In general, ENDOR transitions should exist in the 75-MHz frequency range for the $M_s = \pm\frac{3}{2}$ groups of hyperfine energy levels and in the 25-MHz range for the $M_s = \pm\frac{1}{2}$ levels. However, no transitions were observed in the 25-MHz range. This could be due to insufficient rf power in the ENDOR coil. ENDOR was readily obtained in the 75-MHz range, and fortunately this is sufficient to calculate all the hyperfine parameters in the spin Hamiltonian. Measurements were made in the 75-MHz region in all four alums for the low- and high-field groups of hyperfine lines when the magnetic field was directed along the z and perpendicular directions of a magnetic complex. To verify that the magnetic complexes were indeed axially symmetric, ENDOR measurements were made for various positions of the magnetic field in the perpendicular planes.

Typical chart recordings of the z-axis ENDOR

spectra in the 75-MHz range when the magnetic field is set on each hyperfine line of the $M_s = \frac{3}{2} \rightarrow \frac{1}{2}$ group in $Rb(H_2O)$ alum are shown in Fig. 3. The labeling scheme displayed in Fig. 3 is explained in Fig. 4. The lines marked e are extra lines which have frequency values that are averages of the two lines flanking them. Figure 5 shows the z-axis ENDOR transitions in the 75-MHz range for the $M_s = -\frac{3}{2} \rightarrow -\frac{1}{2}$ group of hyperfine lines in $Rb(D_2O)$ alum. This pattern of ENDOR lines is the same as in the corresponding hyperfine group of $Rb(H_2O)$ alum but the linewidths are greater in the deuterated alum. The ordering of the spacings of the hyperfine energy levels along the z axis, as determined by the intensities and frequencies of the ENDOR lines when the magnetic field is set on the outer two hyperfine lines of a group, is shown in Fig. 6 for $Rb(H_2O)$ alum and in Fig. 7 for $Cs(H_2O)$ alum. It is seen that the ordering is different in the two types of alums. That is, the most intense ENDOR lines for the H_5 and H_8 hyperfine line positions in the $M_s = \frac{3}{2} \rightarrow \frac{1}{2}$ group in $Cs(H_2O)$ alum are obtained at high and low frequencies, respectively, whereas the opposite was the case for $Rb(H_2O)$ alum. Calculations show that the difference can be attributed mostly to an order of magnitude difference in the quadrupole interactions. A similar pattern was obtained for the respective deuterated alums.

The presence of extra ENDOR e transitions was quite clear in the Rb alums, both on the z axis and in the perpendicular direction. In the Cs alums some traces of the extra lines were apparent in the high-field groups of hyperfine lines on the z axis, but at no time were they observed in the low-field groups. Three mechanisms are considered which could cause the extra lines. (i) Forbidden transitions of the type $\Delta M_I = \pm 2$: If the lines are due to this cause then they must have been produced by second harmonics of the rf oscillator. That is, an extra line observed at a frequency labeled e_{1ab} is in reality a transition at twice this frequency. However, this mechanism can probably be ruled out because when the rf oscillator is swept at a frequency of $2e_{1ab}$ no transition is observed. (ii) Double photon absorption: If two photons of frequency e_{1ab} combine then they could cause the observed line. (iii) Transitions caused by a broadened intermediate hyperfine level: A photon of frequency e_{1ab} can be pumped twice between three energy levels if the intermediate level has sufficient broadening so that it spreads appreciably over the midfrequency point of the outer two levels. The nature of the e transitions are under further study.

The method of parameter fitting was done as follows: The values of $g_\parallel$, $g_\perp$, and D were obtained from the ESR measurements. The spin-Hamiltonian matrix including hyperfine interactions was first diagonalized using second-order perturbation theory to give a set of equations which could be solved to give rough values of A, B, Q', $g'_{n\parallel}$, and $g'_{n\perp}$. These values were then used as a starting point for exact diagonalization of the matrix using an IBM 360 computer program. The final values of the parameters including $g_\parallel$, $g_\perp$, and D are given in Table I.

V. DISCUSSION AND CONCLUSIONS

The ENDOR results show that the hyperfine interaction is anisotropic with $A > B$ for the RbGa alums and $A < B$ for the CsGa alums. The analysis also shows that these alums have positive and negative D values, respectively. As the temperature is lowered from 300 to 4.2 °K, the magnitude of D decreases in both types of alums and hence the trigonal distortion is decreased in each case. The magnitude of D changes by about 38% in RbGa

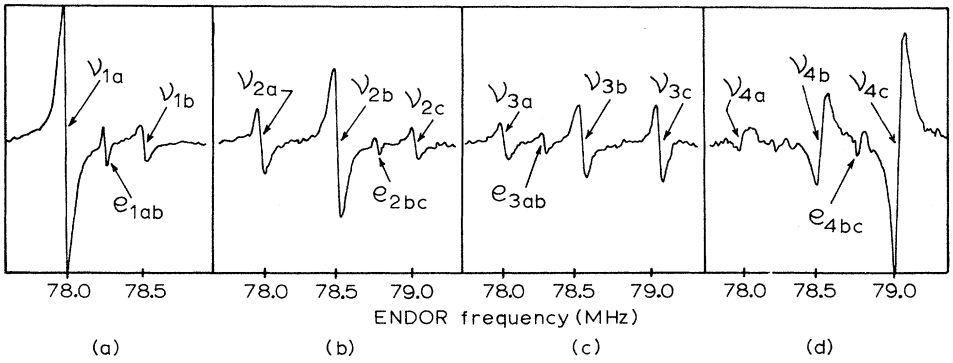

FIG. 3. Typical chart recordings of the z-axis ENDOR spectra of $^{53}Cr^{3+}$ in $RbGa(SO_4)_2 \cdot 12H_2O$ in the 75-MHz frequency range for the $M_s = \frac{3}{2} \rightarrow \frac{1}{2}$ hyperfine lines. The notation is explained in Fig. 4. The spectra are obtained when the magnetic field positions are set on (a) H_1, (b) H_2, (c) H_3, and (d) H_4 as noted in Fig. 4.

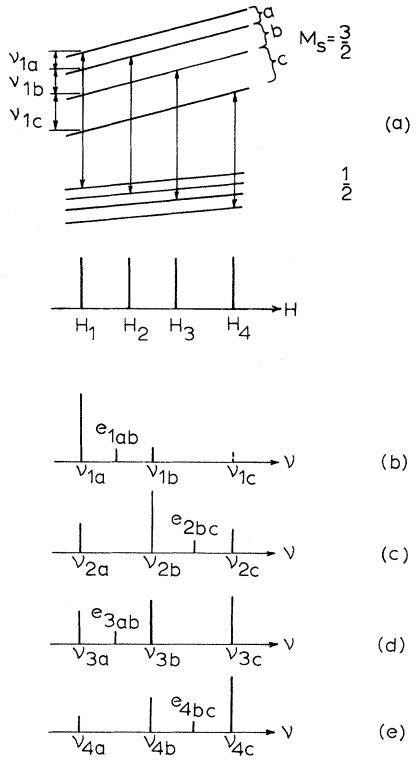

FIG. 4. Diagrammatic representation of (a) the $M_s = \frac{3}{2} \rightarrow \frac{1}{2}$ hyperfine lines of $^{53}Cr^{3+}$ in $RbGa(SO_4)_2 \cdot 12H_2O$. Parts (b), (c), (d), and (e) give the relative intensities and positions of the ENDOR lines obtained when the magnetic field is set at the positions H_1, H_2, H_3, and H_4, respectively. Lines marked e are extra ENDOR lines having frequency values that are averages of the two lines flanking them.

alum and by only 8% in CsGa alum.

McGarvey[7,8] has shown for a trigonally distorted magnetic complex that the combination of $A > B$ and D positive represents a trigonal extension of the octahedron of waters surrounding the Cr^{3+} ion, while the combination of $A < B$ and D negative represents a trigonal compression. These parameter relationships are in fact obtained in the present work for the RbGa alums and CsGa alums, respectively. However, it is not certain in the alums if the distortion is caused by the nearest-neighbor water molecules coordinated to chromium or is due to the direct action of other atoms in the unit cell which are known to be distributed with trigonal symmetry.

The quadrupole interaction constants Q' obtained at 4.2 °K for $Rb(H_2O)$ and $Cs(H_2O)$ alums are -0.0164 (10^{-4} cm^{-1}) and 0.1546 (10^{-4} cm^{-1}), respectively. These values differ by nearly an order of magnitude and both cannot be expected to give the correct value of the nuclear quadrupole moment of ^{53}Cr when utilizing simple formulas such as Eqs. (5) and (7), since these formulas indicate that Q' is proportional to D. To calculate the quadrupole moment of ^{53}Cr from the data one must first determine where the simple formulas can be applied.

Segleken and Torrey[15] performed room-temperature nuclear-magnetic-resonance (NMR) studies on $^{27}Al^{3+}$ in the α-alums $KAl(SO_4)_2 \cdot 12H_2O$ and $NH_4Al(SO_4)_2 \cdot 12H_2O$, and they found a ratio of 1.12 ± 0.03 for the aluminum quadrupole interaction parameters Q'. The authors note that in the chromium isomorphs of these alums (also α type) Bagguley and Griffiths[16] found by ESR a similar ratio of 1.12 ± 0.07 for the ground-state splittings ($2D$) in the corresponding chromic alums. No Q' values have been determined at 300 °K for the gallium or chromium sites in the alums of the present investigation, but it seems likely that a relationship similar to above should hold. In fact we would like to postulate further that the ratio of the Q' values for the chromium sites in the Rb and Cs gallium alums at 300 °K is equal to the ratio

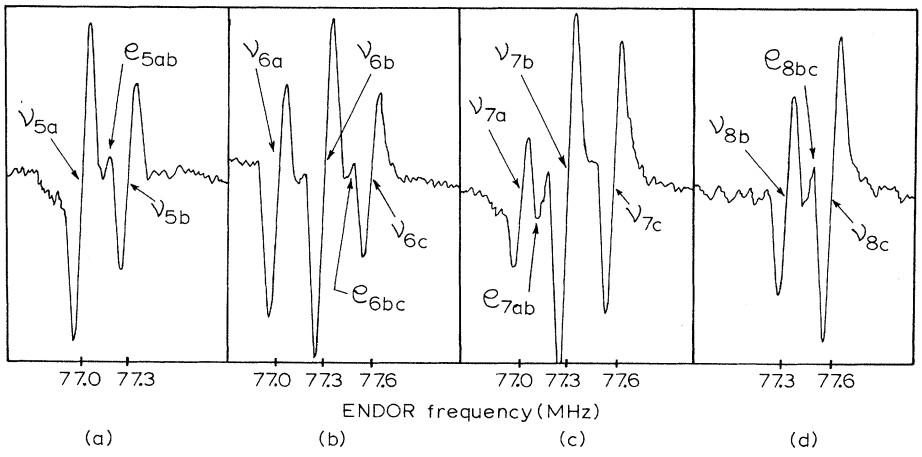

FIG. 5. Typical chart recordings of the z-axis ENDOR spectra of $^{53}Cr^{3+}$ in $RbGa(SO_4)_2 \cdot 12D_2O$ in the 75-MHz frequency range for the $M_s = -\frac{3}{2} \rightarrow -\frac{1}{2}$ hyperfine lines. The spectra are obtained when the magnetic field positions are set on (a) H_5, (b) H_6, (c) H_7, and (d) H_8 as noted in Fig. 6.

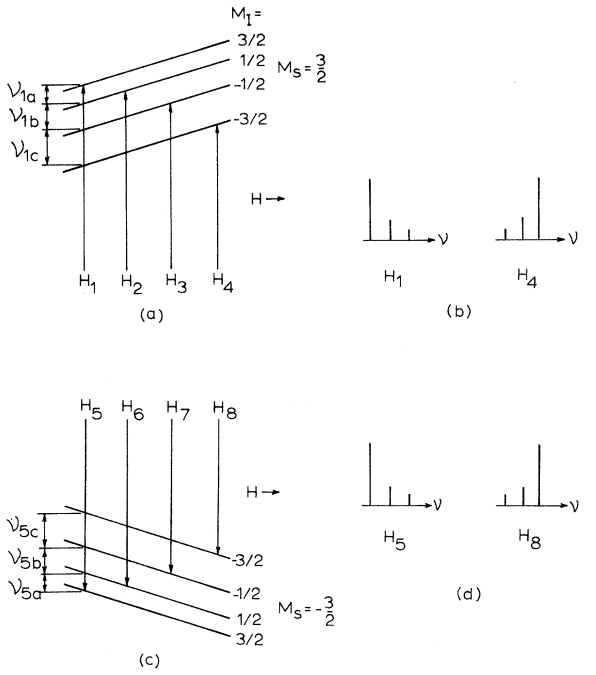

FIG. 6. Ordering of key z-direction ENDOR lines in $RbGa(SO_4)_2 \cdot 12H_2O$: (a) represents the $M_s=\frac{3}{2}\rightarrow\frac{1}{2}$ hyperfine lines and (b) gives the relative positions and intensities of the ENDOR lines obtained when the magnetic field was set at the H_1 and H_4 positions; (c) represents the $M_s=-\frac{3}{2}\rightarrow-\frac{1}{2}$ hyperfine lines and (d) gives the relative positions and intensities of the ENDOR lines obtained when the magnetic field was set at the H_5 and H_8 positions.

of the chromium zero-field splittings. This is expected to be at least a close approximation and it is useful to use it in an attempt to analyze the behavior of the alums as the temperature is lowered to 4.2 °K. The inference here is that the chromium-doped alums behave in a predictable manner at 300 °K and any anomalies occur at low temperatures.

The ratio of the ground-state splittings at 300 °K for Cr^{3+} in $Rb(H_2O)$ and $Cs(H_2O)$ alums is -1.18, and so if we assume that this ratio is equal to the ratio of the respective quadrupole interaction constants, we can write

$$(Q'_{Rb(H_2O)}/Q'_{Cs(H_2O)})_{300\,^\circ K} = -1.18\ . \qquad (8)$$

Burns[13] showed that linear relationships hold between the D values of Cr^{3+} and Q' values of Al^{3+} and Ga^{3+} in $C(NH_2)_3Al(SO_4)_2 \cdot 6H_2O$ (GAlSH) and $C(NH_2)_3Ga(SO_4)_2 \cdot 6H_2O$ (GGaSH) when the temperature is lowered. It is expected that a linear relationship should also hold to a good approximation in the alums for the chromium D and Q' parameters. By expressing the results as a ratio between the two types of alums the following relationship is obtained:

$$\Delta Q'_{Rb(H_2O)}/\Delta Q'_{Cs(H_2O)} = \Delta D_{Rb(H_2O)}/\Delta D_{Cs(H_2O)} = -5.42\ . \qquad (9)$$

Equations (8) and (9) allow room-temperature Q' values for the chromium sites to be predicted. Solving the equations we find

$$\begin{aligned}(Q'_{Rb(H_2O)})_{300\,^\circ K} &= -0.228\times10^{-4}\ cm^{-1}\ ,\\ (Q'_{Cs(H_2O)})_{300\,^\circ K} &= 0.193\times10^{-4}\ cm^{-1}\ .\end{aligned} \qquad (10)$$

The ratio of these values is, of course, -1.18. When the nuclear quadrupole moment (eQ) for ^{53}Cr is calculated from Eqs. (5), (7), and (10), a value of $eQ=-0.040$ b is obtained in each case. In the calculations we have used the Cr^{3+} free-ion values of $\lambda=91\ cm^{-1}$ and $\langle r^2\rangle=1.447$ a.u. [where 1 a.u. $=5.29172\ (10^{-9}$ cm)]. The values of ΔE were measured at 300 °K for the $Rb(H_2O)$ and $Cs(H_2O)$ alums and they were found to be 17 800 and 17 700 cm^{-1}, respectively. The value of $1-\gamma_\infty$ was taken to be 12.0 for Cr^{3+}.

The quadrupole moment of ^{53}Cr can be calculated at 4.2 °K using Eqs. (5) and (7) and the measured

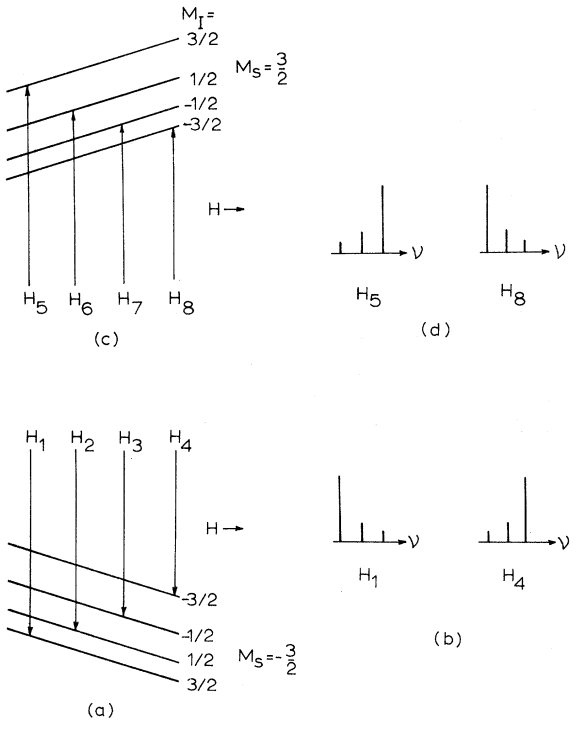

FIG. 7. Ordering of key z-direction ENDOR lines in $CsGa(SO_4)_2 \cdot 12H_2O$: (a) represents the $M_s=-\frac{3}{2}\rightarrow-\frac{1}{2}$ hyperfine lines and (b) gives the relative positions and intensities of the ENDOR lines obtained when the magnetic field was set at the H_1 and H_4 positions; (c) represents the $M_s=\frac{3}{2}\rightarrow\frac{1}{2}$ hyperfine lines and (d) gives the relative positions and intensities of the ENDOR lines obtained when the magnetic field was set at the H_5 and H_8 positions.

TABLE I. Spin-Hamiltonian parameters of $^{53}Cr^{3+}$ in gallium alums.

Spin-Hamiltonian parameter	RbGa alum				CsGa alum			
	300 °K		4.2 °K		300 °K		4.2 °K	
	H_2O	D_2O	H_2O	D_2O	H_2O	D_2O	H_2O	D_2O
$g_\parallel$ (±0.0050)	1.9754	1.9754	1.9751	1.9799	1.9715	1.9746	1.9718	1.9747
$g_\perp$ (±0.0050)	1.9675	1.9653	1.9734	1.9688	1.9694	1.9663	1.9722	1.9696
D (10^{-4} cm^{-1}) (±2.0)	864.7	869.1	534.2	526.7	−731.7	−753.3	−670.1	−698.4
A (MHz) (±0.0020)			52.1167	52.1317			51.6358	51.6596
B (MHz) (±0.0020)			51.8743	51.8908			52.4263	52.4755
Q' (10^{-4} cm^{-1}) (±0.0010)			−0.0164	−0.0165			0.1546	0.1542
g_n' (±0.0010)			−0.3111	−0.3111			−0.3111	−0.3111

values of D and Q'. The room-temperature measurements of ΔE are used in the calculations since they are not expected to change substantially at 4.2 °K. For $Cs(H_2O)$ alum we find $eQ = -0.036$ b and the value for $Rb(H_2O)$ alum is -0.0046 b. Since the value obtained for Cs alum is essentially identical to the predicted room-temperature values found for the Cs and Rb alums we conclude that the quadrupole moment of ^{53}Cr has the value $eQ = -0.035 \pm 0.005$ b. The value of -0.0046 b found at 4.2 °K for $Rb(H_2O)$ is too small by nearly an order of magnitude, so it is concluded that Eq. (7) is not applicable to the Rb alum at low temperature because it predicts the wrong value of V_{zz}. If one assumes that $eQ = -0.035$ b for Rb alum, then from Eq. (5), we find $V_{zz} = 0.152 \times 10^{-4}$ cm^{-1}/b at 4.2 °K. The values of V_{zz} found using Eqs. (7) and (5) for both $Rb(H_2O)$ and $Cs(H_2O)$ alums are plotted in Fig. 8. It appears likely in Rb alum that the large temperature change in D is associated with a complex behavior in V_{zz}.

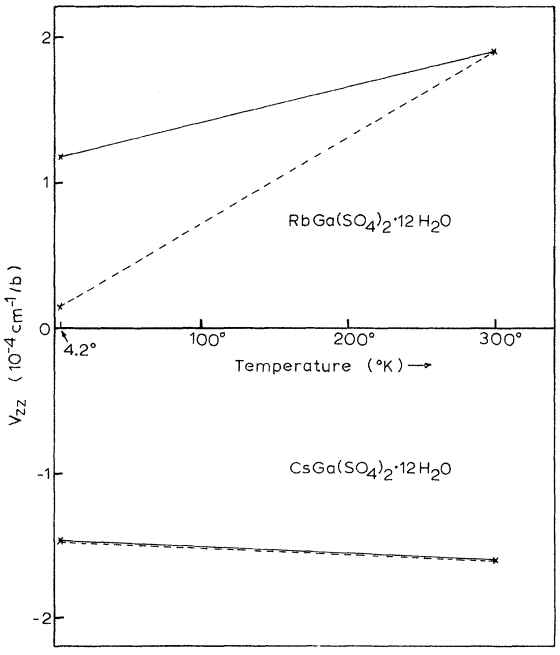

FIG. 8. Plot of V_{zz} against temperature for the chromium magnetic complexes in $RbGa(SO_4)_2 \cdot 12H_2O$ and $CsGa(SO_4)_2 \cdot 12H_2O$. The solid lines are obtained by using Eq. (7), while the dotted lines are obtained by using Eq. (5) and assuming that $eQ = -0.035$ b.

The only other experimental value of the nuclear quadrupole moment of ^{53}Cr reported was that of Terhune *et al.*[2] from ENDOR studies in ruby. They found a value of -0.03 b in essential agreement with our value. However, the agreement is fortuitous because incorrect assumptions were made in the case of ruby. The analysis consisted of comparing the quadrupole interaction constants of the Cr^{3+} and Al^{3+} sites in ruby using Eq. (5) and then assuming that V_{zz} was the same in both sites. They also assumed that $1 - \gamma_\infty = 6.0$ for Cr^{3+}, whereas the best value is now known to be 12.0 ± 1. If their analysis is redone using $eQ = -0.035$ b, $1 - \gamma_\infty = 12.0$ for Cr^{3+}, and $eQ = 0.149$ b, $1 - \gamma_\infty = 3.36$ for Al^{3+}, one finds V_{zz} (Al site) $= 2.4\, V_{zz}$ (Cr site) in ruby. The nega-

tive sign of eQ for ^{53}Cr is verified in our work since only this sign will allow the experimental results to be fitted to the spin Hamiltonian.

The nuclear Zeeman interaction was isotropic in each of the alums studied, and the effective nuclear g value was found to be $g'_{n\parallel} = g_{n\perp} = -0.3111 \pm 0.0005$ in each case. This interaction contributed about 1.0 and 0.5 MHz, respectively, to the splittings of the energy levels at the high and low magnetic field positions of the hyperfine lines along the z axes. These splittings are large enough to be readily measured by ENDOR. Using the Cr^{3+} free-ion values of $\lambda = 91$ cm^{-1}, $\langle 1/r^3 \rangle = 3.959$ a.u., and taking the average value of $\Delta g = -0.028$ one finds the shielding factor from Eq. (6) to be $\sigma = 0.0072$. The nuclear g value is then calculated to be $g_n = g'_n/(1+\sigma) = -0.3090$. The nuclear magnetic moment is given by $\mu_n = g_n I$ nuclear magnetons, and so if $I = \frac{3}{2}$ we find $\mu_n = -0.4640\ \mu_N$ for ^{53}Cr. This can be compared to a handbook value[17] of $\mu_n = -0.4735\ \mu_N$ obtained by NMR of ^{53}Cr in solution. The deviation between the two values is outside experimental error and the lack of agreement is unexplained. However, it is generally recognized that the value of μ_n can best be determined independently from NMR measurements. ENDOR measurements of μ_n for ^{53}Cr in MgO [18] and ruby[2] give values in essential agreement with the handbook value, but these measurements were made in a narrow region of magnetic field, whereas our measurements spanned a region of over 2000 G. It is possible that the narrow region allows more freedom in fitting the g'_n parameter than was possible in our work.

ACKNOWLEDGMENTS

The authors would like to thank the National Research Council, Ottawa, Canada, for financial assistance. One of us (A.G.D.) would also like to thank the Ontario Government for the student fellowships received during the course of the work.

[1]R. W. Terhune, J. Lambe, G. Makhov, and L. G. Cross, Phys. Rev. Letters 4, 234 (1960).

[2]R. W. Terhune, J. Lambe, C. Kikuchi, and J. Baker, Phys. Rev. 123, 1265 (1961).

[3]J. O. Artman and J. C. Murphy, Phys. Rev. 135, A1622 (1964).

[4]J. O. Artman, Phys. Rev. 143, 541 (1966).

[5]A. Danilov and A. Manoogian, preceding paper, Phys. Rev. B 6, 4097 (1972).

[6]H. Weaver, Varian Associates Seventh Annual NMR-EPR Workshop Notes, 1963 (unpublished).

[7]B. R. McGarvey, J. Chem. Phys. 40, 809 (1964).

[8]B. R. McGarvey, J. Chem. Phys. 41, 3743 (1964).

[9]R. M. Sternheimer (private communication).

[10]R. M. Sternheimer, Phys. Rev. 146, 140 (1966).

[11]S. Geschwind, *Hyperfine Interactions*, edited by A. J. Freeman and R. B. Frankel (Academic, New York, 1967), p. 243.

[12]D. E. O'Reilly and T. Tsang, Phys. Rev. 157, 417 (1967).

[13]G. Burns, Phys. Rev. 123, 1634 (1964).

[14]W. M. Walsh, Jr., Phys. Rev. 114, 1473 (1959); 114, 1485 (1959).

[15]W. G. Segleken and H. C. Torrey, Phys. Rev. 98, 1537 (1955).

[16]D. M. S. Bagguley and J. H. E. Griffiths, Proc. Roy. Soc. (London) A204, 188 (1950).

[17]*Handbook of Chemistry and Physics* (The Chemical Rubber Co., Cleveland, Ohio, 1965).

[18]G. A. Woonton and G. L. Dyer, Can. J. Phys. 45, 2265 (1967).